Research article

Jan Dupuis* and Heiner Kuhlmann

High-Precision Surface Inspection: Uncertainty Evaluation within an Accuracy Range of 15µm with Triangulation-based Laser Line Scanners

Abstract: Triangulation-based range sensors, e.g. laser line scanners, are used for high-precision geometrical acquisition of free-form surfaces, for reverse engineering tasks or quality management. In contrast to classical tactile measuring devices, these scanners generate a great amount of 3D-points in a short period of time and enable the inspection of soft materials. However, for accurate measurements, a number of aspects have to be considered to minimize measurement uncertainties. This study outlines possible sources of uncertainties during the measurement process regarding the scanner warm-up, the impact of laser power and exposure time as well as scanner's reaction to areas of discontinuity, e.g. edges. All experiments were performed using a fixed scanner position to avoid effects resulting from imaging geometry. The results show a significant dependence of measurement accuracy on the correct adaption of exposure time as a function of surface reflectivity and laser power. Additionally, it is illustrated that surface structure as well as edges can cause significant systematic uncertainties.

Keywords: high precision laser scanning, laser line scanner, laser triangulation, measurement uncertainties

DOI: 10.1515/jag-2014-0001

received: January 02, 2014; accepted: February 24, 2014

1 Introduction

The geometrical acquisition of free-form surfaces for reverse engineering or quality management has a great need in manufacturing process. In the recent years, laser scanning has become more important in this field of work [1, 4, 18]. Thereby, the required accuracy is commonly in order of a hundredth of millimetre or better. These close-up laser scanners use laser triangulation and are mounted on computer numerical control (CNC) machines [4] or articulated measuring arms [10]. Such combinations enable a high-resolution, fast and non-invasive three dimensional acquisition of free-form surfaces. The advantage of laser scanning compared to conventional tactile measuring systems is the great amount of 3D data points that are collectable in a short period of time. Additionally, the contactless measuring process enables the inspection of soft or flexible materials [17]. However, there are also disadvantages. Today's triangulation-based laser line scanners are usually one order of magnitude less accurate compared to tactile probes [25]. Furthermore, the optical characteristics of the surface material as well as an unadapted imaging geometry can influence the measuring process and cause both higher noise and systematic uncertainties.

Over the last years, several studies have shown the importance of the analysis of measurement uncertainties [3, 7, 11, 15, 20, 21, 22, 23, 24]. Thus, Xi et al. [24] indicated that various scanner-to-surface distances and inclination angles raise systematic uncertainties for the used sensor. They used a combination of a planar and a spherical reference artifact to locate random and systematic effects. Based on the resulting uncertainties, they generated a calibration function and successfully applied it to different scans of spherical test bodies.

A similar effect was also detected by Isheil et al. [11]. They used an identical artifact for uncertainty verification but additionally included the roll-angle to calculate a calibration function in matrix form.

Vukasinovic et al. [21, 22, 23] examined the impact of different measuring angles and scanner-to-surface distances on the number of acquired points and the measuring noise. Different from Xi and Isheil [24, 11], they determined a prediction-function with the goal to evaluate the number of points and the measuring noise for any imaging geometry.

A different approach was presented by Van Gestel et al. [20]. They designed a performance evaluation test for laser line scanners mounted on coordinate measuring machines (CMMs), which is an easy, fast and representative technique for most of the measuring tasks. The test procedure

***Corresponding Author: Jan Dupuis:** Institute of Geodesy and Geoinformation, University of Bonn, Nussallee 17, 53115 Bonn, Germany, E-mail: dupuis@igg.uni-bonn.de

Heiner Kuhlmann: Institute of Geodesy and Geoinformation, University of Bonn, Nussallee 17, 53115 Bonn, Germany

is based on plane measurements using different imaging geometries regarding inclination angles and scanner-to-surface distance. Hence, it is possible for any user to evaluate the inner accuracy of the measuring system easily.

Guidi et al. [7] also presented a performance evaluation test for triangulation-based range sensors. The test was performed on low-cost test artifacts with sensors of different resolution and accuracy dimensions (< 0.4 mm). In addition to Van Gestel et al. [20], they used artifacts with absolute geometry features like spheres or cones to evaluate an absolute overall accuracy.

While the previous approaches were primarily focused on the imaging geometry or fast and easy performance tests, Muralikrishnan et al. [15] exposed and analyzed so-called "hidden performance attributes" (Businaki et al. [3]) of a laser triangulation spot probe. For example, they demonstrated the influence of different surface materials on linearity and highlighted the impact on height measurements of two different ceramic gauges. They also took into account the finite size of the laser-spot and displayed its impact on various measurement scenarios.

In summary, it can be stated that most of the studies only regarded external impacts on measurement accuracy caused by imaging geometry providing that all sensor parameters are chosen optimally. However, measurements within an accuracy range close to the accuracy limit of the sensor requires a detailed knowledge of all possible uncertainty sources. Considering the measurement process with a triangulation-based laser line scanner, a lot of internal and external uncertainty sources can be identified that are not yet addressed in detail.

The aim of this paper is to demonstrate and evaluate possible sources of measurement uncertainties during the measurement process independent of the imaging geometry. The study focuses the interaction between laser power, exposure time and surface reflectivity and analyzes the impact on the measurement accuracy. Additionally, the scanner's warm-up behavior and its reaction to areas of discontinuity, e.g. edges and different surface materials, are illustrated.

The paper is organized as follows: Section 2 gives a short introduction to the operating principle of laser line scanners. Afterwards, the measurement setup, the test artifact as well as the algorithms used for point cloud analysis are presented in Section 3 and 4. In Section 5, all experiments and results are illustrated together. Finally, all results are summarized and discussed in Section 6.

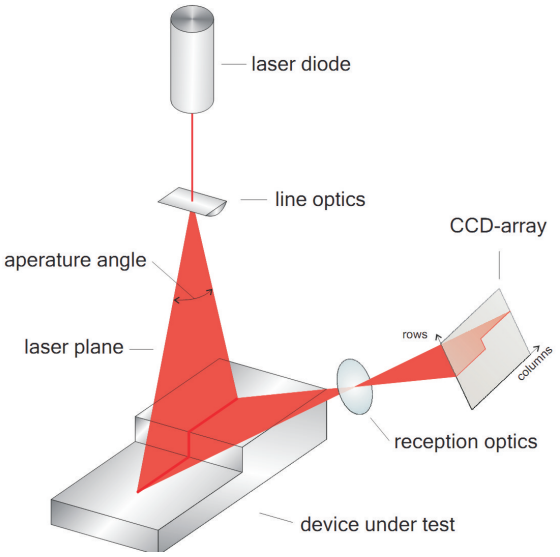

Fig. 1. Principle of light-section-method.

2 Operating principle of laser line scanners

Triangulation-based measurement systems principally yield the distance between the object's surface and sensor's reference point [5]. Laser line scanners, which represent a generalization of classical point-based laser triangulation sensors, work according to the light-section method (Figure 1). Thus, it is possible to acquire the 2-dimensional contour of a surface.

Therefore, a laser line is projected onto the object's surface. The back-scattered laser light is collected by the reception optic and imaged on a CCD-array (Charged-Coupled-Device). To ensure a sharp image of the laser line over the entire measuring range, the assembly of the CCD-array has to meet the so-called "Scheimpflug"-condition [5]. Finally, the profile of the measured surface can be derived from the contour of the received laser line on the CCD. Thereby, the number of columns of the CCD indicates the number of points per profile while the rows are linked to the sensor-to-surface distance (Figure 1) by the sensor's characteristics function. To obtain a precise distance measurement, the exact row-position of the laser line has to be evaluated. Because of their physical finite width, the laser line is commonly represented by multiple pixels for each column. For this reason, the center of mass (CoM) of the contour line has to be calculated by a "subpixel estimation". Different basic approaches [6, 16] can be found for this purpose. The quality of the calculated center eminently depends on the shape and the intensity distribu-

tion of the received laser line. In an ideal case, the back-scattered laser line should have a Gaussian intensity distribution. However, in practice, the shape of the received signal primarily depends on two main factors.

First of all, the physical width of the laser line on the object's surface is closely linked to the emitted laser power combined with the reflective properties of the measured surface. I.e. the higher the laser power, the wider the laser line appears on the object's surface.

The second impact on the laser line's shape is the exposure time of the CCD-array. Analogous to customary digital cameras, the amount of collected laser light is coupled to the exposure time. Using a long exposure time leads to an enlargement of the received laser line on the CCD-chip and could additionally result in an entire saturation of single pixels. This in turn results in a lower accuracy of the estimated CoM. It can be concluded that for precise measurements laser power and exposure time have to be adapted dependent on the surface characteristics of the measured object (Section 5.2).

In addition to these sensor specific properties, external factors such as different surface materials or points of discontinuity (e.g. edges) can also influence the laser line's shape and cause measurement uncertainties (Sections 5.3 and 5.4).

3 Measurement Setup

The measurement system used consists of the *scanCONTROL 2700-100* laser line scanner form *MicroEpsilon* company (hereafter "scanner") combined with a linear horizontal actuator from *Isel* company (hereafter "support") (Figure 2).

The scanner gathers 640 points per profile with a point-to-point distance between 0.138 – 0.175 mm depending on the scanner-to-surface distance. In vertical direction, the measurement accuracy, specified by the manufacturer, is ± 0.015 mm (1σ), considering optimal measuring conditions using the MicroEpsilon standard target [13].

The support enables a point-to-point distance of 0.012 mm in the direction of movement with a positioning accuracy of ± 0.003 mm (1σ). However, preliminary investigations of the movement exposed vertical uncertainties in a maximum range of ± 0.01 mm, due to a limited quality of the guidance system. To reduce uncertainties caused by movement of the support, the scanner is fixed above the measurement-slide, i.e. the measuring object is moved through the laser plane. Thus, z- and y-axes are aligned to scanners' laser plane directions (z = vertical; y || laser line), while the x-axis is aligned to the movement direction of the support (Figure 2). On that condition, the measurement uncertainty of the whole measurement system can be prescribed to ± 0.02 mm (1σ), in accordance with the GUM (**G**uide to the Expression of **U**ncertainty in **M**easurement) [2].

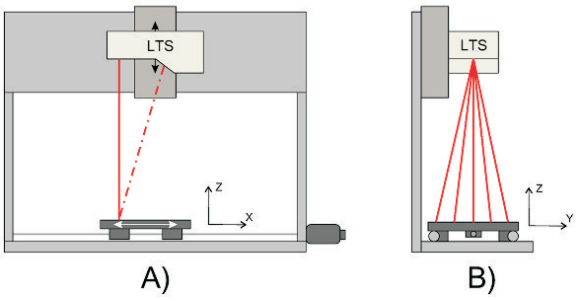

Fig. 2. Measurement Setup: **A)** front view, **B)** side view, (LTS = Laser Triangulation Sensor).

4 Reference artifact and point cloud analysis

In the following experiments, a high-precision planar artifact manufactured by the AIMESS company was used. This reference plane is made of special white ceramics with reflective properties optimized for laser measurements. The machined surface has a certified planarity of 1.5 μm.

For analysis, the resulting point cloud is approximated by a best-fit plane in accordance with the least-square-method. In detail, a four-parameter approach is used for the plane's parametrization

$$\boldsymbol{F(L, X)} = A(x_i + v_{xi}) + B(y_i + v_{yi}) + C(z_i + v_{zi}) + D = \mathbf{0}, \quad (1)$$

where A, B, C and D describe the plane's parameter, x_i, y_i and z_i are the observations and v the residuals. Because eq. (1) can be multiplied by an arbitrary nonzero number, there is a manifold of solutions. For this reason, the following constraint is adopted to the approach:

$$\boldsymbol{y(x)} = \sqrt{A^2 + B^2 + C^2} = 1 \quad (2)$$

The four parameters of the plane are estimated by minimizing the residuals according to the least-square principle

$$\mathbf{v}^{\mathbf{T}}\Sigma_{\mathbf{ll}}^{-\mathbf{1}}\mathbf{v} \rightarrow \mathbf{min}. \quad (3)$$

where $\Sigma_{\mathbf{ll}}$ represents the covariance matrix of the observations. This results in a non-linear Gauss-Helmert-model and a total system of normal equations [14]. Due to the

standardization of the surface normal vector (eq. (2)), the dimension of the normal equation system does not increase with the amount of data points, but is reduced to five. This enables the approximation of point clouds with hundreds of thousands of points with low computational costs.

The solution of a non-linear problem has to be transferred to a linear case using linearization. However, a linearization at the approximate situation $(\mathbf{0}, \mathbf{X^0})$ merely leads to an approximate solution [12]. Because of that, for a rigorous solution, linearization has to be performed at the approximate situation $(\mathbf{v^0}, \mathbf{X^0})$ [12]. This finally leads to the corrected linear condition equation

$$\mathbf{f}(\mathbf{v^0}, \mathbf{X^0}) = \mathbf{B}(\mathbf{v} - \mathbf{v^0}) + \mathbf{A}(\mathbf{X} - \mathbf{X^0}) + \mathbf{w_1} = \mathbf{0} \tag{4}$$

under condition

$$\mathbf{g}(\mathbf{X^0}) = \mathbf{C}(\mathbf{X} - \mathbf{X^0}) + \mathbf{w_2} = \mathbf{1}. \tag{5}$$

Therein, $\mathbf{A}$ and $\mathbf{B}$ are coefficient matrices containing the partial derivatives of eq. (1) w.r.t. the parameters and the residuals respectively and $\mathbf{C}$ is the coefficient matrix containing the partial derivatives of eq. (2) w.r.t. the parameters. $\mathbf{w_1}$ and $\mathbf{w_2}$ describe the discrepancy vectors. If the normal equation matrix is invertible, surcharges to approximate solution could be calculated using established procedures.

Looking at the stochastic model, all observations are assumed to be uncorrelated and have the same weight which leads to following covariance matrix:

$$\boldsymbol{\Sigma_{ll}} = \sigma^2 \boldsymbol{Q_{ll}} = \sigma^2 \boldsymbol{I}. \tag{6}$$

In equation (6) $\mathbf{Q_{ll}}$ is the cofactormatrix and $\mathbf{I}$ represents the identity matrix.

The following experiments generally used the posteriori standard deviation

$$\hat{\sigma_0} = \sqrt{\frac{\boldsymbol{v^T \Sigma_{ll}^{-1} v}}{r}} \tag{7}$$

where r describes the redundancy and the Euclidean distance of the point cloud w.r.t. the best-fit plane for the measure of accuracy.

5 Experiments

In this Section the realized experiments and their results are illustrated. First of all, in Section 5.1 the impact of the scanner's warm-up behavior to the accuracy is described. Section 5.2 covers the interaction of surface reflectivity, laser power and exposure time and the influence on the measurement noise. In Section 5.3 the effects coming from different surface structures are presented as well as the scanner's reaction to edges in Section 5.4.

5.1 Warm-up test

For accurate measurements, it is absolutely necessary that a possible warm-up behavior is not reflected in the measurement results. On the part of the manufacturer, a warm-up time of 20 minutes has to be observed. To indicate the effects, which could arise if this warm-up time is disregarded, the reference plane is measured repeatedly at an interval of 3 minutes. All scanner properties are chosen "optimal" (Section 5.2) and kept constant for uniform measurement conditions. 15 measurements of 1:45 minutes each were accomplished, which represents a period of 71 minutes in total.

Since the effect could be both random or systematic, in addition to posteriori standard deviation, the CoM of the whole point cloud is taken into account as presented in [20]. Therefore, the distance in direction of the surface normal between the CoMs regarding the first measurement is calculated:

$$D_{1j} = \mathbf{n_1} \circ (\bar{\mathbf{x}}_\mathbf{1} - \bar{\mathbf{x}}_\mathbf{j}) \tag{8}$$

Therein, $\mathbf{x_j}$ denotes the CoM of the j–th point cloud while $\mathbf{n_1}$ signifies the surface normal of the first measured point cloud. Based on these values, possible systematic effects in distance measurement could be detected.

Considering the results in Figure 3, it can be clearly seen that the CoM is moving in vertical direction, i.e. the sensor's warm-up behavior influences the distance measurement systematically. The dashed line in Figure 3 indicates the reachable accuracy of 0.015 mm (1σ) specified by the manufacturer [13]. Distance variations underneath this limit cannot be resolved reliably and could be considered as non-significant. Based on this, it can be shown that this limit is reached after a warm-up period of about 20 minutes. Significant variations in standard deviation were not determined in the measurement series.

5.2 Influence of exposure time and laser power

As mentioned in Section 2, the quality of the distance measurements is strongly influenced by the shape and the intensity distribution of the received laser line. Basically, there are three main impact factors influencing these attributes:

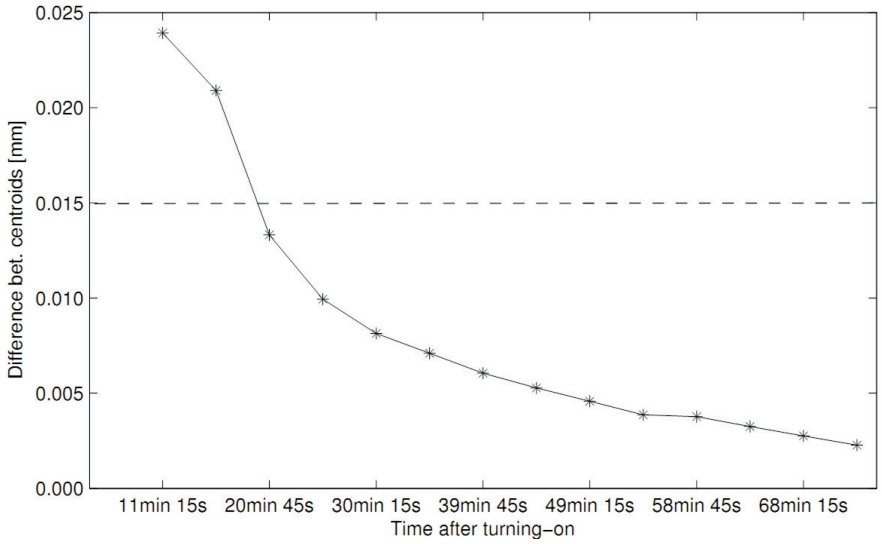

Fig. 3. Difference between sequenced point clouds.

1. The emitted laser power,
2. the surface reflectivity, and
3. the exposure time of the reception-sensor.

Because of the invariance of the surface reflectivity, the only way to control the line characteristic is the adaption of both laser power and exposure time depending on the optical properties of the surface. Before starting a measurement, these scanner properties have to be adapted to the current measuring conditions.

In the following, the impact of exposure time and laser power as well as the one of unsuitable scanner properties on the resulting point cloud should be demonstrated. Therefore the aforementioned reference plane is measured using different scanner attributes. The scanning results are analyzed by using the posteriori standard deviation and the distance of the point-cloud w.r.t. the best-fitting plane. For further interpretation, the width of the laser line on the CCD-chip and the averaged intensity of the point cloud are regarded. The intensity describes the maximum amount (relative) of back-scattered laser light collected in CCD-elements for every measured point. If the intensity reaches 95% or higher, the CCD-chip is overexposed and the CCD-elements are entirely saturated.

The scanner provides a variation of the laser power in two classes: low (2 – 3 mW) and high (10 mW). Furthermore, the exposure time of the CCD-array can be adjusted between 0.01 – 40 ms.

First of all, the measurements were performed using low laser power. Therefore, the reference plane is scanned repeatedly using different exposure times varying from 0.35 up to 1.3 ms with an increment of 0.05 ms. The minimum exposure limit was chosen to be the first exposure time which produces a complete point cloud without underexposed line-pixels, while the maximum limit represents an entire saturation of the CCD-array elements of the laser line. In Figure 4, the resulting standard deviations are illustrated as a function of exposure time, showing the standard deviation decreases from 0.018 mm at 0.35 ms to 0.010 mm at an exposure time of 1 ms.

However, the magnitude of these results needs to be interpreted with caution. Considering the prescribed accuracy of ± 0.02 mm (1σ) of the whole measurement system, the minimum posteriori standard deviation of approximately 0.010 mm is significantly lower. This phenomenon is caused by an inappropriate stochastic model. All measured points representing the planar artifacts are assumed to be uncorrelated (eq. (6)). For this reason and because of a very high amount of 3D-points (approximately 100.000), the posteriori standard deviation of the best-fit plane is constantly too optimistic. However, using consistent measuring conditions, the resulting process can be seen as representative, with the restriction that the magnitude of standard deviation could be certainly higher.

The averaged intensity of the received signal at the point of minimum standard deviation is about 92%. Figure 4 shows that the standard deviation slightly increases for exposure times above 1 ms. Regarding the deviations from the best-fit plane (Figure 5), it can be illustrated that

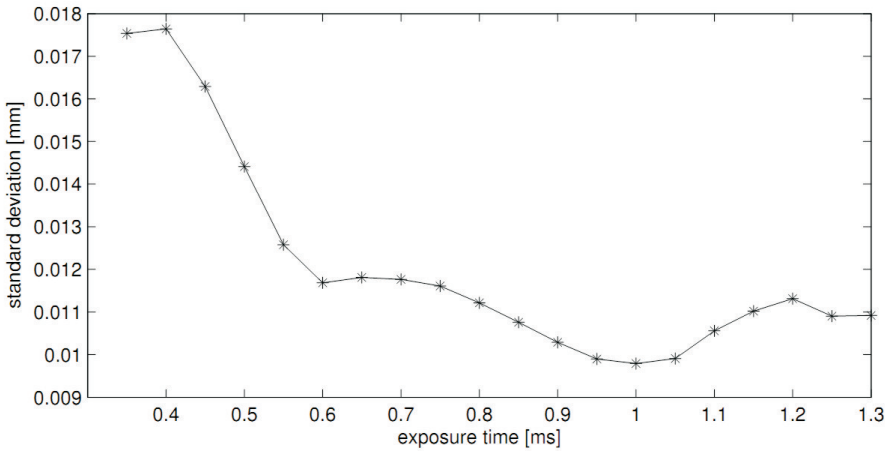

Fig. 4. Posteriori standard deviation (averaged over multiple measurement series) for different exposure times scanned with low laser lower.

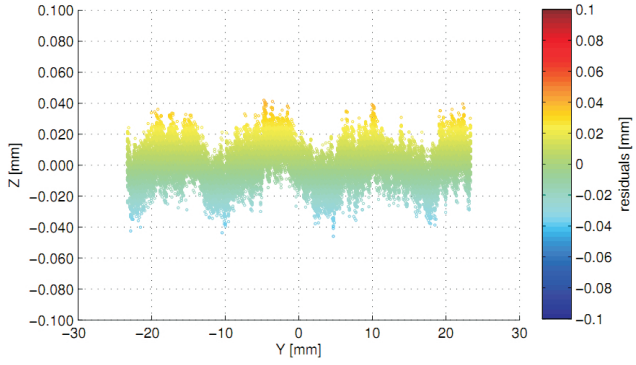

Fig. 5. Point cloud of the plane gauge for averaged intensity of 95%. The perspective is rotated to y-z-plane (parallel to laser plane) with the direction of view aligned to x-axis (moving direction).

using an exposure time that is too long causes systematic uncertainties in the resulting point cloud.

These undulate deviations arise when the intensity of the received laser line reaches about 95%, which corresponds to saturation of the CCD-array elements. From a physical point of view, in the case of overexposure, the accumulated charge is able to fill adjacent pixels ("blooming"-effect) [9]. Additionally, this effect could be reinforced by integration of charge during the CCD's readout ("smear"-effect) [9]. The impact of these effects is associated with the columns of the CCD-array, thus both effects could affect the distance measurement.

In a second step, similar measurements were performed using high laser power. In contrast to the previous experiment with low laser power, the exposure time has to be adjusted more precisely. The range between an incomplete point cloud and an overexposed CCD-chip merely covers 0.17 ms. For this reason, the exposure time was incremented with a step size of 0.01 ms, from 0.1 ms up to 0.27 ms.

The results generally feature a similar behavior as shown for low laser power. The lowest standard deviation of 0.016 mm was also reached at an intensity of about 92% and nearly the same laser line width as obtained for low laser power. Nevertheless, the calculated posteriori standard deviation was about one third greater. An explanation of this phenomenon can be found by a detailed analysis of the received laser line on the CCD-chip. Therefore, a small section (16 × 31 pixels) of the CCD-image was extracted and is presented in Figure 6. To ensure a better interpretability, the reference plane's surface was aligned with the scanner's y-axis (Figure 2) with the result that the received laser line is imaged horizontally on the CCD-array.

Figure 6 **A** illustrates that the imaged laser line consists of one main pixel line with an intensity of 92% and two side lines with constant lower intensity in case of a low laser power. Using high laser power (Figure 6 **B**) leads to significantly more noisy side lines. Thus, subpixel estimation is affected negatively resulting in a more noisy point cloud.

Corresponding to the result with low laser power, systematic deviations as presented in Figure 5 were also found using high laser power and long exposure times.

Summing up, the results illustrated the importance of an accurate adaption of the scanner setting to the actual scanning situation. It was presented that inadequate scan-

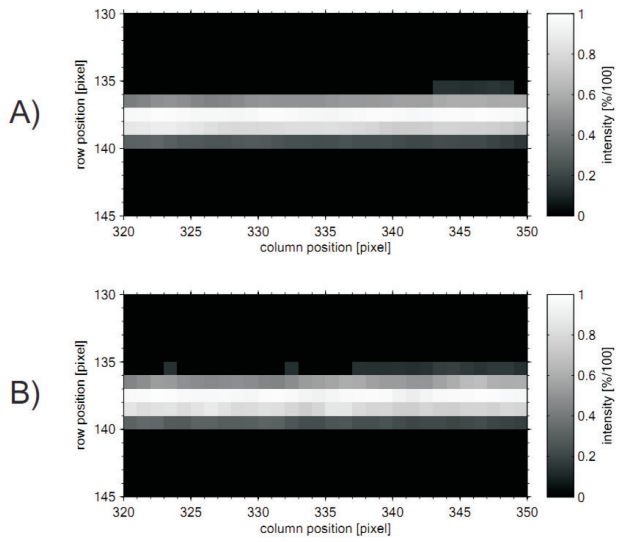

Fig. 6. Image section of the received laser line at an intensity of 92%: **A)** low laser power, **B)** high laser power.

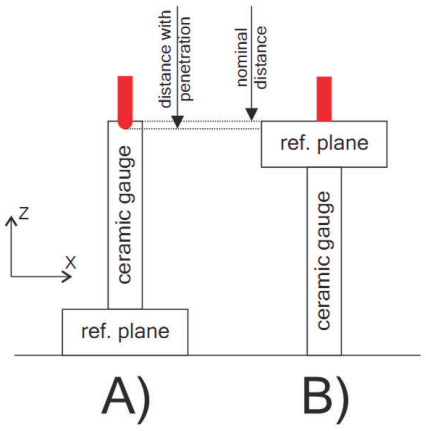

Fig. 7. Measurement setup for the estimation of surface penetration: **A)** distance w.r.t. ceramic gauge's surface, **B)** distance w.r.t. reference plane's surface.

ner settings cause significant random and systematic uncertainties. For highest accuracy, the exposure time and the laser power should be set to level, where the received laser line is projected preferably thin and imaged with an intensity of nearly 92%.

5.3 Impact of surface structure to accuracy

In this section, the impact of surface characteristics on the resulting point cloud accuracy should be illustrated. As already known from terrestrial laser scanners, surface characteristics of different materials, like styrofoam, can provoke uncertainties due to penetration of laser light into the surface structure [8, 19]. This effect primarily results in a distance measurement that is systematically too long. A similar impact could be expected for triangulation-based line scanners. The penetration of the laser into the surface structure causes a laser line on the CCD that is back-scattered form different distances. This leads to an enlargement and a displacement of the received laser line on the CCD-array, which in turn results in a displaced CoM and higher measurement noise, due to more inaccurate subpixel estimation.

To illustrate the impact of surface penetration on measurement noise, a planar artifact made of marble was scanned using both provided laser powers and at an intensity of approximately 92%. For comparability reasons, measurements were performed using the same measuring window and nearly the same scanner-to-surface distance that were used in Section 5.2. As predicted, resulting standard deviations are consistently greater, despite the use of the optimal intensity for data acquisition (Table 1). The reason is the width of the received laser line. As presented in Table 1, the imaged laser line is enlarged to the doubled size compared to an optically optimized surface when scanning marble. Because of the larger width, the subpixel estimation is more sensitive to small changes in the intensity distribution. This can be seen from the results of a scan with high laser power. Comparable to the results in Section 5.2, the posteriori standard deviation increased significantly caused by more noisy side lines in the received signal.

In an additional experiment, the impact of surface penetration to the distance measurement is demonstrated. Therefore, in a first step, a gauge block made of conventional ceramics is set on top of the reference plane (Figure 7 **A**) and the distance to the scanner is acquired. In a second step, the arrangement of the test bodies is changed in a way that the distance is measured with respect to the reference plane's surface (Figure 7 **B**). The difference between both offsets should be almost zero as long as the laser is back-scattered from top of surfaces. However, in contrast to the special ceramics of the reference plane, conventional ceramics do not prevent surface penetration. In this case, the difference between the measured offsets equals the systematic effect, caused by the penetration of the laser into the surface structure. Repeated distance measurements resulted in difference of 0.030 mm.

Table 1. Comparison of standard deviations (std. dev.) of different surface materials.

object	laser pw.	std. dev.	intensity	line width
ceramic ref.	low	10 μm	92%	4 px
plane	high	16μm		
marble ref.	low	15μm	92%	10 px
plane	high	28μm		

By means of the experiments, it can be demonstrated that penetrable surface structures cause significant uncertainties in terms of higher measurement noise and a systematically too long distance measurement.

5.4 Impact of edges on resulting 3D-points

A further reason for uncertainties is attributed to edges. Edges cause significant systematic uncertainties due to the finite width of laser. In case of terrestrial laser scanners, this effect mostly provokes the rounding of edges or produces so called comet's tails, because the signal is reflected by the object's surface as well as by surfaces behind [19]. Consequently, the sensor receives a mixed signal from different surfaces which evokes a systematic deviation in the distance measurement [8].

The situation is slightly different when using a triangulation-based laser scanner. Principally, laser line scanners are as well affected by edges, with the difference that the main uncertainties are not referable to multiple reflections. Instead, the characteristics of the laser line influences the resulting distance measurement. The quality of the calculated distance is directly linked to the quality of subpixel estimation, which in turn depends on the laser line's characteristics. In case of an edge, only a part of the transmitted signal is received by the sensor matrix (Figure 8), resulting in a non-Gaussian intensity distribution.

For this reason, the estimated CoM of the laser line is displaced and the distance is calculated inaccurately. Additionally, Figure 8 **B** and **C** show that the effect depends on the direction of edge regarding the scanner orientation. This results in different directions of uncertainties. In case of Figure 8 **B**, the distance will be measured too short whereas in case of Figure 8 **C** it will be measured too long.

To demonstrate the magnitude of the resulting deviations, circular ceramic platelets were scanned. These thin platelets have a highly accurate planarity and sharp edges comparable to the reference plane with the advantage, that different orientations between laser plane and edge can be simulated concerning the circular form.

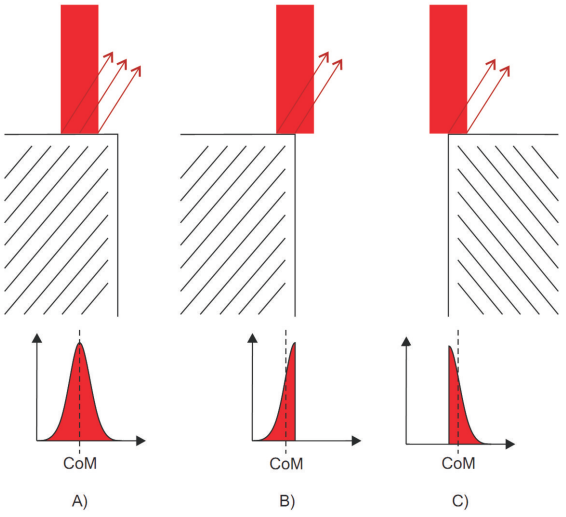

Fig. 8. Intensity distribution of the received laser line on CCD-chip while scanning A) a surface, or B + C) edges from different scanning directions.

Figure 9 shows the resulting point cloud of platelets measurements. The excepted impact on distance measurement occurs with a magnitude up to −0.5 mm in case of parallel orientation between edge and laser line. Moreover, the results show that the magnitude of deviations approaches zero for an angle of 90° between laser line and edge.

A similar effect also emerges on the transition between bright and dark surfaces. If the exposure time is adjusted with respect to the bright, well reflecting surface, the CCD-array will collect only little or no laser light from the dark surface. Looking at the transition point, this leads to a non-Gaussian intensity distribution causing the same uncertainties as described previously.

The experiment pointed out that edges cause significant systematic uncertainties with a magnitude up to several tenth of a millimeter. Furthermore, the effect depends on the relative orientation of the laser line and the edge.

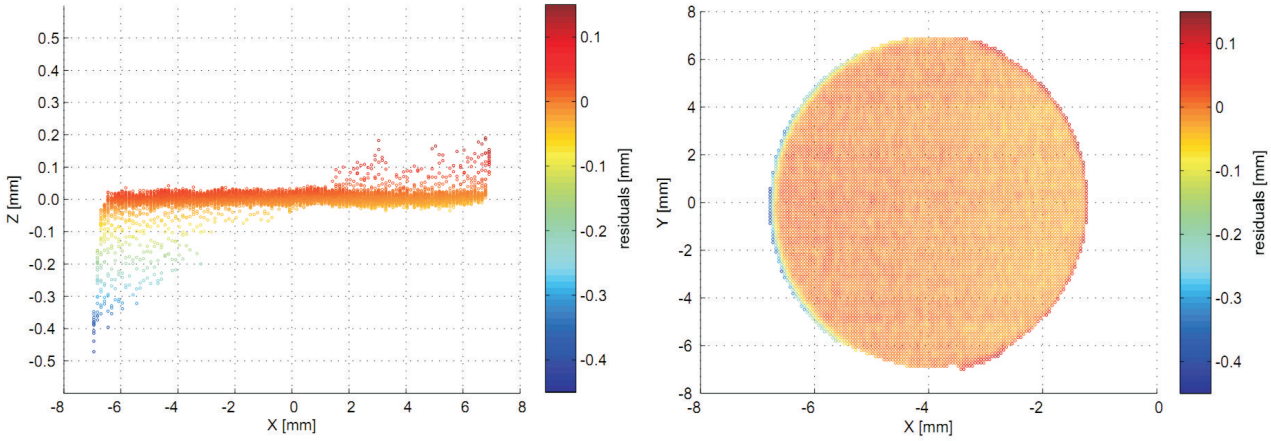

Fig. 9. Resulting point cloud of circular platelets. The scan direction was from left to right, i.e. the left edge equals Fig. 8 *C)* and the right one equals *B)*.

6 Conclusion and Outlook

This study proposes that already small deviations from the ideal scanner settings or slight changes of the surface structure have a significant impact on the measurement accuracy. The most remarkable result is that measurement accuracy is directly linked to the adjustment of laser power and exposure time depending on the surface characteristics. Thereby, the smallest uncertainties resulted at an averaged intensity of the received signal of 92%. While exposure times that were too short only increased the measurement noise, systematic uncertainties emerged when exposure times were used that were too long.

Even the surface structure itself can cause significant uncertainties due to penetration of the laser. The resulting random and systematic uncertainties are ineliminalbe and therefore have to be considered in terms of accuracy rating.

Another reason for the uncertainties is attributed to edges. Scanning an edge leads to systematic uncertainties with a magnitude up to several tenth of a millimeter depending on the relative orientation of the edge and the laser line.

All these effects become more important in practical use. To minimize the measurement uncertainties, all scanner settings have to be adopted to the object's surface. Especially objects with different reflective surface properties have to be treated with caution. In this case, exposure time and laser power should be adjusted automatically (if possible) or set to a level that avoids saturation of the CCD-array to prevent systematic uncertainties.

If highest precision is requested and the accuracy should be pre-estimated, a detailed knowledge of the surface characteristics will be necessary to capture all uncertainty-sources.

Furthermore, the results of the edge experiment indicated that smallest uncertainties arise for an orthogonal alignment of the laser line w.r.t. the edge direction. Planning a measurement path should consider this effect.

The current study was limited by the use of planar artifacts for uncertainty investigation. These artifacts only enable the estimation of the inner accuracy of the sensor. Measuring absolute values, e.g. step sizes, additionally requires a good knowledge of linearity of the sensor, which has not been studied in detail yet.

The presented effects were identified by the use of a single sensor, but can be treated as generally applicable. Since the magnitude is probably sensor-specific, similar experiments should be performed using other triangulation-based line scanners.

Acknowledgement: The authors want to express their gratitude to thank Birgit Kretschmann, Stefan Paulus and Christoph Holst for proofreading. Furthermore, the authors are deeply grateful to Dr.-Ing. Wolfgang Schauerte for the suggestions and the support during the experiments and the interpretation of the measurement data.

References

[1] Bi Z. M. and Wang L., Advances in 3D data acquisition and processing for industrial applications, *Robotics and Computer-Integrated Manufacturing* 26 (2010), 403–413.

[2] Bureau International des Poids et Mesures, Evaluation of Measurement Data - Guide to the Expression of Uncertainty in Mea-

surement, *Joint Committee for Guides in Metrology 100:2008* (2008).

[3] Businaki M., Levine A. and Stevenson W. H., Performance Characteristics of Range Sensors utilizing Optical Triangulation, *Aerospace and Electronics Conference, 1992, NAECON 1992, Proceedings of the IEEE 1992 National*, 1230-1236, 1992.

[4] Cheng W.-L. and Menq C.-H., Integrated Laser/CMM System for the Dimensional Inspection of Objects Made of Soft Material, *The International Journal of Advanced Manufacturing Technology* 10 (1995), 36–45.

[5] Donges A. and Noll R., *Lasermeßtechnik. Grundlagen und Anwendungen*, Hüthig Verlag, Heidelberg, 1993.

[6] Forest J., Teixidor J. M., Salvi J. and Cabruja E., A Proposal for Laser Scanners Sub-pixel Accuracy Peak Detector, *Workshop on European Scientific and Industrial Collaboration*, 525-532, Mickolc (Hungria), 2003.

[7] Guidi G., Russo M., Magrassi G. and Bordegoni M., Performance evaluation of triangulation based range sensors, *Sensors* 10 (2010), 7192–7215, MDPI AG, Basel, Switzerland, 2010.

[8] Gordon B., *Zur Bestimmung von Messunsicherheiten terrestrischer Laserscanner*, Ph.D. thesis, TU Darmstadt, 2008.

[9] Luhmann T., *Nahbereichsphotogrammetrie: Grundlagen - Methoden - Anwendungen*, pp. 179–180, Wichmann Berlin, 2010.

[10] Hexagon Metrology ROMER Division, *ROMER Infinite 2.0: Neue Maßstäbe in Ergonomie und Genauigkeit*, 2009, http://cnc-auction.de/kataloge/xx7088.pdf.

[11] Isheil A., Gonnet J.-P., Joannic D. and Fontaine J.-F., Systematic error correction of a 3D laser scanning measurement device, *Optics and Lasers in Engineering* 49 (2011), 16–24.

[12] Lenzmann L. and Lenzmann E., Strenge Auswertung des nichtlinearen Gauß-Helmert-Modells, *AVN* 2 (2004), 68–73.

[13] MICRO-EPSILON Messtechnik GmbH & Co. KG, *scanCONTROL: 2D/3D Laser-Scanner (Laser-Profil-Sensoren)*, http://www.micro-epsilon.de/download/products/_dimension/dax--scanCONTROL-27x0--de.html.

[14] Mikhail E. M. and Ackermann F., *Observations and least squares*, Dun-Donelly, New York, 1976.

[15] Muralikrishnan B., Ren W., Everett D., Stanfield E. and Doiron T., Performance evaluation experiments on a laser spot triangulation probe, *Measurement* 45 (2012), 333–343.

[16] Naidu D. K. and Fisher R. B., A Comparative Analysis of Algorithms for Determining the Peak Position of a Stripe to Sub-pixel Accuracy, *British Machine Vision Conference 1991*, 217–225, Springer London, 1991.

[17] Paulus S., Behmann J., Mahlein A.-K., Plümer L. and Kuhlmann H., Low-Cost 3D Systems: Suitable Tools for Plant Phenotyping, *Sensors* 14 (2014), 3001–3018.

[18] Sansoni G., Trebeschi M. and Docchio F., State-of-The-Art and Applications of 3D Imaging Sensors in Industry, Cultural Heritage, Medicine, and Criminal Investigation, *Sensors* 9 (2009), 568–601.

[19] Van Genechten B., Quintero M. S., De Bruyne M., Poelman R., Hankar M., Barnes S., Caner H., Budei L., Heine E., Reiner H., Garcia J. L. L. and Taronger J. M. B., *Theory and practice on Terrestrial Laser Scanning*, Universidad Politécuica de Valencia, Editorial UPV, 2008, 28–34.

[20] Van Gestel N., Cuypers S., Bleys P. and Kruth J.-P., A performance evaluation test for laser line scanners on CMMs, *Optics and Lasers in Engineering* 47 (2009), 336–342.

[21] Vukašinović N., Bračun D., Možina J. and Duhovnik J., The influence of incident angle, object colour and distance on CNC laser scanning, *The International Journal of Advanced Manufacturing Technology* 50 (2010), 265–274.

[22] Vukašinović N., Bračun D., Možina J. and Duhovnik J., A new method for defining the measurement-uncertainty model of CNC laser-triangulation scanner, *The International Journal of Advanced Manufacturing Technology* 58 (2012), 1097–1104.

[23] Vukašinović N., Možina J. and Duhovnik J., Correlation between Incident Angle, Measurement Distance, Object Colour and the Number of Acquired Points at CNC Laser Scanning, *Strojniški vestnik - Journal of Mechanical Engineering* 58 (2012), 23–28.

[24] Xi F. and Liu Y. and Feng H.-Y., Error Compensation for Three-Dimensional Line Laser Scanning Data, *The International Journal of Advanced Manufacturing Technology* 18 (2001), 211–216.

[25] Zeiss Calypso, Marktübersicht "Taktile CNC-3D-Koordinatenmessmaschinen", *Fertigung* 4 (2012).